Minigenes encoding N-terminal domains of human cardiac myosin light chain-1 improve heart function of transgenic rats

Hannelore Haase,* Gisela Dobbernack,* Gisela Tünnemann,*,‡ Peter Karczewski,* Cristina Cardoso,* Daria Petzhold,* Wolfgang-Peter Schlegel,* Steffen Lutter,* Petra Pierschalek,* Joachim Behlke,* and Ingo Morano*,†,[1]

*Max-Delbrück-Center for Molecular Medicine, Berlin, Germany; †Charité University Medicine, Johannes-Müller-Institute for Physiology, Berlin, Germany; and ‡Franz-Volhard-Clinics, Berlin, Germany

ABSTRACT **In this study we investigated whether the expression of N-terminal myosin light chain-1 (MLC-1) peptides could improve the intrinsic contractility of the whole heart. We generated transgenic rats (TGR) that overexpressed minigenes encoding the N-terminal 15 amino acids of human atrial MLC-1 (TGR/hALC-1/1–15, lines 7475 and 3966) or human ventricular MLC-1 (TGR/hVLC-1/1–15, lines 6113 and 6114) isoforms in cardiomyocytes. Synthetic N-terminal peptides revealed specific actin binding, with a significantly ($P<0.01$) lower dissociation constant (K_D) for the hVLC-1/1–15-actin complex compared with the K_D value of the hALC-1/1–15-actin complex. Using synthetic hVLC-1/1–15 as a TAT fusion peptide labeled with the fluorochrome TAMRA, we observed specific accumulation of the N-terminal MLC-1 peptide at the sarcomere predominantly within the actin-containing I-band, but also within the actin-myosin overlap zone (A-band) in intact adult cardiomyocytes. For the first time we show that the expression of N-terminal human MLC-1 peptides in TGR (range: 3–6 μM) correlated positively with significant ($P<0.001$) improvements of the intrinsic contractile state of the isolated perfused heart (Langendorff mode): systolic force generation, as well as the rates of both force generation and relaxation, rose in TGR lines that expressed the transgenic human MLC-1 peptide, but not in a TGR line with undetectable transgene expression levels. The positive inotropic effect of MLC-1 peptides occurred in the absence of a hypertrophic response. Thus, expression of N-terminal domains of MLC-1 represent a valuable tool for the treatment of the failing heart.–Haase, H., Dobbernack, G., Tünnemann, G., Karczewski, P., Cardoso, C., Petzhold, D., Schlegel, W.-P., Lutter, S., Pierschalek, P., Behlke, J. Morano, I. Minigenes encoding N-terminal domains of human cardiac myosin light chain-1 improve heart function of transgenic rats. *FASEB J.* 20, 865–873 (2006)**

Key Words: myosin light chain · actin · heart · contractility · rat

HEART FAILURE, a state of reduced contractile function, represents a leading cause of human morbidity and mortality. It affects 7,000,000 individuals per year, and accounts for annual costs of 10–40 billion dollars in the U.S. (1). Conventional treatment with drugs leaves a poor prognosis for patients with symptomatic heart failure: ~45% die within a year (2), worse than for most forms of cancer. Therefore, the development of alternative concepts and drugs for the treatment of heart failure is a major challenge of our modern civilization. Cardiac contraction is driven by the interaction of the motor domain of the heavy chains (MHC) of type II myosin with actin (3). Different myosin light chain (MLC) isoforms are noncovalently associated with an α-helical "neck" distal from the motor domain, namely, essential (MLC-1) and regulatory (MLC-2) MLC (4). The NH_2 terminus of all MLC-1 isoforms of vertebrate striated muscle consists of a repetitive Ala-Pro rich elongated rod segment with an antenna-like flexibility (5–11) (residues 15–30) protruding a highly interactive "sticky" element at the most NH_2 terminus, which contains several charged amino acid residues (12, 13). The sticky NH_2 terminus, but not the Ala-Pro rod, of MLC-1 (14, 15) binds to the C-terminal residues 360–364 of actin (16, 17). There are two MLC-1 genes in the human heart, encoding an atrial-specific (hALC-1) and a ventricular-specific (hVLC-1) isoform (12,13).

Actin binding of the NH_2 terminus of MLC-1 slows down myosin motor function *in vitro* (9, 14, 18–24). Likewise, weakening the MLC-1-actin interaction by N-terminal MLC-1 peptides, which competitively bind to actin, increased motor activity *in vitro* (14, 15, 25, 26). Tropomyosin increased the affinity of N-terminal MLC-1 peptides to F-actin, while binding of troponin I abolished MLC-1 peptide binding to F-actin-tropomyosin (19, 27). This could explain the Ca^{2+} dependency of MLC-1 binding to regulated actin (19), since Ca^{2+}

[1]Correspondence: Max-Delbrück-Center for Molecular Medicine, Molecular Muscle Physiology, Robert-Rössle-Str. 10, 13125 Berlin, Germany. E-mail: imorano@mdc-berlin.de

doi: 10.1096/fj.05-5414com

binding to troponin C reduced actin affinity of troponin I (28) and therefore may lose its inhibitory effect on MLC-1 binding to actin during muscle activation. Furthermore, in the presence of Ca^{2+}, a more extended conformation of the NH_2 terminus of MLC-1 occurs, making this domain more susceptible to papain cleavage (29), and a much tighter binding to actin could be observed (30).

Hence, myosin motor activity, and therefore contractility of the whole heart, may be experimentally and therapeutically improved by manipulation of the interaction between the NH_2 terminus of MLC-1 and actin: inhibition of MLC-1/actin interaction, i.e., by N-terminal MLC-1 peptides, should accelerate myosin activity, thus improving cardiac contraction. To test this hypothesis, we generated transgenic rats (TGR) harboring minigenes encoding N-terminal human cardiac MLC-1 peptides and compared the contractility of isolated perfused Langendorff hearts of non-TGR with TGR.

We demonstrate here that the N-terminal domain 1–15 of both human atrial and ventricular MLC-1 isoforms specifically bind to actin *in vitro* and rapidly associate with the sarcomeres of the living primary adult cardiomyocyte. The specific actin binding capacity of these N-terminal MLC-1 peptides was associated with a pronounced improvement of the intrinsic contractile state of the isolated perfused heart of those TGR lines that expressed the transgenic peptides. Non-expressing TGR revealed normal contraction.

The direct improvement of myosin motor function of the heart by manipulation of MLC-1/actin interaction on application of functional N-terminal domains of MLC-1 may represent a novel alternative concept for the treatment of heart failure.

MATERIALS AND METHODS

Analysis of actin binding of synthetic MLC-1 peptides

N-terminal human VLC-1 and ALC-1 peptides 1–15 with or without flanking TAT and conjugated TAMRA fluorochrome were chemically synthesized, purified by HPLC, and controlled by MALDI-TOF commercially (Biosyntan, Berlin, Germany). Binding studies between cardiac G-actin and synthetic N-terminal hALC-1 and hVLC-1 peptides 1–15 were performed in an XL-A type analytical ultracentrifuge (Beckman, Palo Alto, CA, USA) equipped with UV absorbance optics. Sedimentation equilibrium of different molar ratios peptide/actin was reached after 2 h of overspeed at 24,000 rpm, followed by an equilibrium speed of 20.000 rpm for ~26 h at 10°C. Depending on the loading concentration of the radial, absorbance in each compartment was recorded at three different wavelengths between 230 and 240 nm using molar absorbance coefficients. Molecular mass determinations employed the global fit of three radial distributions described by equation 1:

$$A_r = A_{rm}\, e^{MF} \text{ with } F = [(1 - \rho\,\nu)\omega^2\,(r^2 - r_m^2)]/2RT \quad [1]$$

Using the program Polymole (33) in this equation, ρ is the solvent density, ν is the partial specific vol, ω is the angular velocity, R is the gas constant, and T is the absolute temperature. A_r means the radial absorbance and A_{rm} represents the corresponding value at meniscus position. Determination of molecular mass and analyzing absorbance profiles at three different wave lengths allowed estimation of the partial concentration of the reactants and complex. Dissociation constants and stoichiometry for the reacting components were derived from the sum of exponentials (radial concentration distribution curves) considering molecular mass, loading concentration, and extinction coefficients of the reactants as described (33). Determination of dissociation constants of the actin/petide complexes were performed in 1 mM KH2PO2, 3 mM NaHPO4, 0.1 mM ATP, pH 7.4. G-actin was purchased from Cytoskeleton (Denver, CO, USA) and centrifuged by 100,000 *g* for 1 h to eliminate F-actin contaminations. Molecular mass of the peptides were determined by sedimentation velocity experiments at 50,000 rpm and 20°C allowing the simultaneous estimation of sedimentation (s) and diffusion coefficient (D) using approximate solutions of the Lamm equation (34).

Isolation of adult rat cardiomyocytes

Male WKY rats aged 3 months were anesthetized with isofluran followed by intraperitoneal (i.p.) injection of 8 μg xylazine and 35 μg ketamine. Hearts were rapidly removed, transferred into isotonic NaCl solution containing heparin (1000 U), and connected to a cannula of a Langendorff perfusion system. Hearts were perfused at 37°C for 5 min with Ca^{2+}-free with Krebs Henseleit buffer (KHB) and 10 mM butanedione monoxime (BDM) gassed with carbogen. Then perfusion was switched to recirculation with KHB containing 0.04% collagenase (Worthington, Freehold, NJ, USA), 0.2% BSA, and 10 mM BDM for 30 min at 37°C. The ventricles were minced, incubated in the digestion medium (10 min, 37°C), filtered (200 μm pore size), centrifuged, and the cardiomyocytes resuspended in Ca^{2+}-free medium. Ca^{2+} concentration was stepwise increased to 1 mM to obtain Ca^{2+}-tolerant cardiomyocytes. After final washes, cardiomyocytes were resuspended in M199 medium completed with 0.2% BSA, 5% fetal calf serum, 5 mM creatine, 5 mM taurine, 2 mM carnitine, 10 μM cytosine-D-arabinofuranoside, and antibiotics.

Analysis of intracellular peptide localization by laser scanning confocal microscopy

To infect adult primary cardiomyocytes with N-terminal MLC-1 peptides, the human VLC-1 1–15 peptide was associated with the protein transduction domain of TAT protein (italics) from HIV and conjugated with the fluorescence marker 5-tetramethylrhodamine (TAMRA) (MAPKKPEPKK-DDAKAPA*GRKKRRQRRR*-C(5-TAMRA-ME)-amide) (hVLC-1-TAT^{TAMRA}) (Biosyntan, Berlin, Germany). For live cell microsopy isolated cardiomyocytes were placed into a laminin-coated μ-slide 8-well ibiTreat chamber (ibidi) and the peptide hVLC-1-TAT^{TAMRA} was added directly to the HBSS buffer and gently shaken (final concentration 10 μM). Confocal images were acquired on a Zeiss LSM 510 Meta using a 100× phase contrast oil-immersion plan-neofluoar objective 100×/NA1.3. For TAMRA detection of the hVLC-1-TAT^{TAMRA} peptide, the fluorophore was excited at 543 nm and detected with a 565–615 nm band pass filter. Image analysis was performed with the Zeiss LSM Image Examiner Version 3.2 software.

Generation of transgenic rats

We generated two groups of transgenic rats (TGR) that overexpressed minigenes encoding for the N-terminal 15 amino acids of human ALC-1 (TGR/hALC-1/1–15) or human VLC-1 (TGR/hVLC-1/1–15). Two lines were generated for each transgenic group. For production of the transgene constructs, we cloned synthetic cDNA, consisting of the Kozak sequence (GCCACC) in front of the cDNA sequence encoding the first N-terminal 15 amino acids of hALC-1 or hVLC-1, and a stop codon. These synthetic cDNA were cloned downstream of the rat α-myosin heavy chain promoter, followed by the polyadenylation signal of SV40 in pBlueskript II SK. The final 1.242kb transgene construct was linearized with *Xba*I, purified by agarose gel electrophoresis, and used to generate transgenic rats as described (35) with the exception that oocytes from inbred Wistar-Kyoto (WKY) rats were used for pronuclear microinjection. Subsequent founders were crossed with the WKY genetic background and the resulting offsprings breeded to homozygosity.

Genotyping by polymerase chain reaction (PCR)

To identify the animals harboring the transgene, genomic DNA was prepared from tail biopsies and investigated by Southern blot and PCR. DNA was digested with *Hind*III, separated by 1% agarose gels, and hybridized with a ^{32}P-labeled dCTP 60 bp probe derived from *Hind*III digestion of the respective transgene constructs. In the PCR we used a forward primer located in the α-MHC promoter upstream of the 5′ cap signal and a reverse primer located in the transgene coding region, leading to a predicted cDNA product size of 607 bp for TGR/hALC-1–1-15 and 807 bp for TGR/hVLC-1–1-15.

Analysis of mRNA expression by PCR

Transgene expression was investigated on the mRNA concentration by RT-PCR. DNA-free RNA was purified using a commercially available kit (Omniscript RT Kit, Quiagen, Hilden, Germany) from the left ventricle of TGR/hALC-1/1–15, TGR/hVLC-1/1–15, and control WKY. We used random primer as well as poly(T) primer (Operon Biotechnologies, Köln, Germany) to transcribe RNA into cDNA. hALC-1/1–15, and hVLC-1/1–15 cDNA were amplified in the PCR using specific primer pairs (hALC-1/1–15: forward primer: GGAAGTTCTCGGTGGCAGGA (nt749–768I), reverse primer: TTGGCTGCCTCCTTCTTAGG (nt1083–1102; hVLC-1/1–15: forward primer. GGAAGTTCTCGGTGGCAGGA (nt749–768); reverse primer TGGCATCATCCTTCTTGGGC (nt1083–1102) leading to predicted cDNA products of 354 bp that were verified by agarose electrophoresis. Location of the forward primer was downstream of the 5′-cap-signal of the α-MHC promoter.

Analysis of peptide expression by Western blot

Left ventricular tissue was homogenized in a buffer containing 5% SDS, 50 mM Tris, 250 mM sucrose, 75 mM urea, 1 mM EGTA, 1 mM EDTA, 10 mM DTT, pH 7.5, subjected to SDS gradient gel electrophoresis (5–15%) using Ready Gel tris-tricine/peptide gels (Bio-Rad, Hercules, CA, USA), and blotted to a PVC membrane (pore size 0.2 μm; Millipore, Schwalbach, Germany). Peptide-specific antibodies of hALC-1/3–15 and hVLC-1/3–15 were raised in rabbits by immunization with synthetic peptides coupled to keyhole limpet hemocyanin according to standard protocols, then affinity-purified on the respective peptide antigen columns. Synthetic peptides were used as standards for the evaluation of *in vivo* peptide expression of the TGR lines. A highly sensitive chemiluminescence kit (Millipore, Schwalbach, Germany) was used for detection.

Analysis of the contractility of isolated perfused heart preparations

Animal experiments were performed using 12-wk-old transgenic (TGR) rats and age-matched wild type WKY rats. Rats were kept on a 12 h light-dark cycle with 55% humidity at an ambient temperature of 23 ± 2°C and given food and tap water *ad libitum*. The studies were approved by the institutional animal care in the state of Berlin, Germany. Hearts from anesthetized (30 mg/kg sodium chaloralhydrate) and heparinized (500 U/kg) 12-wk-old male transgenic and WKY rats were excised after thoracotomy and cannulated for retrograde aortic perfusion with a modified Krebs-Henseleit solution containing (mM) NaCl (118), KCl (4.7), $CaCl_2$ (1.5), $MgSO_4$ (1.2), $NaHCO_3$ (25), Na_2EDTA 0.05, KH_2PO_4, (0.23), glucose (11.1), and 1 μM albumin. The solution was saturated with 95% O_2/5% CO_2 pH 7.4. The perfusion apparatus was from Hugo-Sachs Electronic (March-Hugstetten, Germany) and the corresponding software was MEM Notocord (Croissy sur Seine, France). Systolic pressure was measured with a latex balloon, filled with ethanol/H_2O (1:1) inserted into the left ventricle through the left atrium via a catheter to a transducer (Isotec, Des Plaines, IL, USA). The pressure in the balloon was set from 14 to 18 mm Hg. The perfusion was carried out at 37°C with a constant aortic pressure of 70 mmHg. After a period of 10 min in which the hearts contracted with their spontaneous frequency, stimulation frequency was fixed at 340 beats/min and the contraction monitored for another 15 min, during which they reached a steady-state contraction.

From the recorded developed isovolumetric left ventricular pressure (LVP) signal, we calculated maximal rate of isovolumetric pressure increase (+dP/dtmax) and maximal rate of isovolumetric pressure decrease (−dP/dtmax) as contractility parameters.

Statistics

Values are expressed as means ± SE, with the number of animals/hearts investigated in parentheses. Student's *t* test was used for significance analysis.

RESULTS

The specific complex formation of synthetic N-terminal peptides with cardiac G-actin was investigated by sedimentation equilibrium ultracentrifugation analysis. We observed a specific interaction between cardiac G-actin and N-terminal peptides 1–15 derived from both the human atrial (hALC-1/1–15), and the human ventricular (hVLC-1/1–15) MLC-1 sequence (**Fig. 1**). We observed a significantly ($P<0.01$) lower dissociation constant (K_D) for the synthetic hVLC-1/1–15-actin complex (24.6±2.2 μM; mean±SE, 9 measurements) compared with the K_D value of the hALC-1/1–15-actin complex (54±2.8; mean±SE, 7 measurements) (Fig. 1). No complex formation was obtained with cardiac G-actin and the corresponding scrambled peptides.

A prerequisite for the biological activity of the N-terminal MLC-1 peptides is their accumulation within

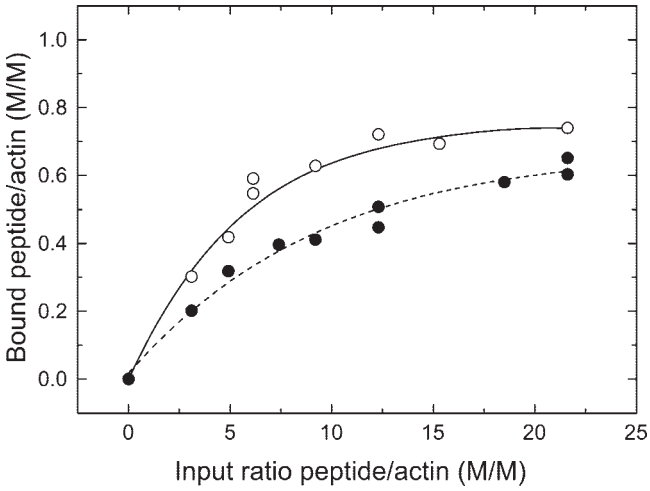

Figure 1. Sedimentation equilibrium ultracentrifugation analysis of the dissociation constants of cardiac G-actin with synthetic hALC-1/1–15 (filled) and hVLC-1/1–15 peptides (open circles).

the sarcomeres of the myofibrils as well as their specific binding to sarcomeric actin in the living cardiomyocyte. Due to the cross-reactivity of our peptide-directed antibodies with endogenous essential myosin light chains, we could not directly detect the transgenic peptides in the cardiomyocytes of the heart of TGR. We therefore incubated freshly prepared resting adult primary rat cardiomyocytes prepared from WKY rats with synthetic hVLC-1/1–15 as a TAT fusion peptide labeled with the fluorochrome TAMRA (hVLC-1-TAT^{TAMRA}) (**Fig. 2**). The hVLC-1-TAT^{TAMRA} (10 μM) rapidly (within minutes) penetrated the cardiomyocytes with an infection efficiency of 100% of the cardiomyocytes. hVLC-1-TAT^{TAMRA} accumulated predominantly in the sarcomeres, in particular within the actin-containing I-band, but considerable fluorescence signals could also be detected in the actin-myosin filament overlap zone (A-band) (Fig. 2). Densitometric analysis of the fluorescence signals along the linescan shown in Fig. 2 revealed arbitrary optical density (OD) values of 92.1 ± 14.7 (66.9%) of hVLC-1-TAT^{TAMRA} accumulated in the I-band (mean±SE of 5 I-bands), while 45.5 ± 5 (33.1%) arbitrary OD values accumulated in the A-band (mean±SE of 5 A-bands). Similar evaluation of the fluorescence distribution within the sarcomeres of 6 primary cardiomyocytes incubated with hVLC-1-TAT^{TAMRA} revealed that 65.8 ± 1.5% of the whole fluorescence signals reside within the I-band ($P<0.001$, compared with the A-band). This localization pattern is specific to

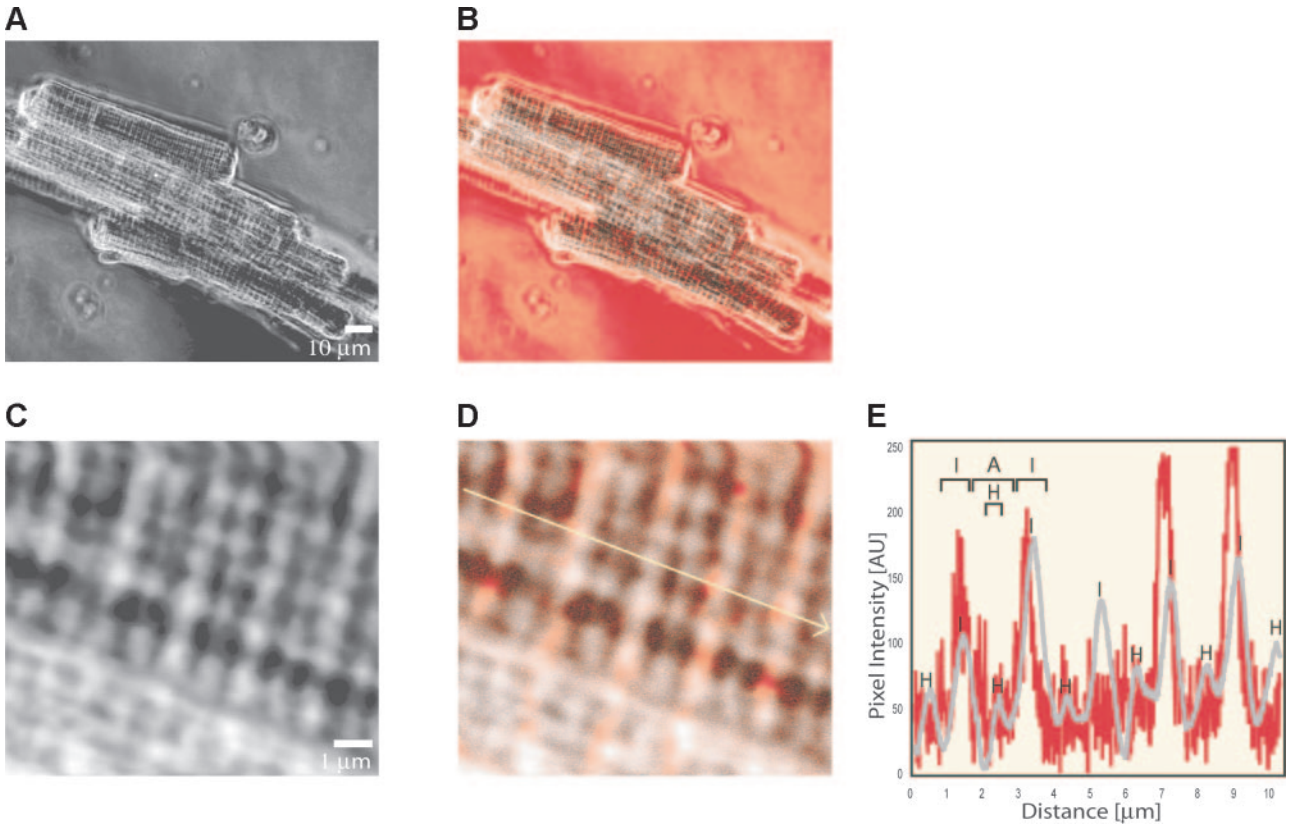

Figure 2. Intracellular localization ot the transduced peptide hVLC-1-TAT^{TAMRA} in living isolated cardiomyocytes: Cardiomyocytes internalized hVLC-1-TAT^{TAMRA} (10 μM) within 2 min after application. *A)* phase contrast and *B)* merge of TAMRA labeled peptide (in red) and phase contrast. *C)* High magnification phase contrast image. *D)* Merge of the hVLC-1-TAT^{TAMRA} and phase contrast at high magnification revealed a regular accumulation of the hVLC-1-TAT^{TAMRA} peptide at the I-bands (higher intensity spots in the phase contrast) but not the A-bands or H-zone. The arrow defines the region of the linescan. *E)* Linescan displaying the pixel intensities of TAMRA-fluorescence (red line) in comparison with the phase-contrast (gray line) in longitudinal direction demonstrating the association of the hVLC-1-TAT^{TAMRA} peptide exclusively within the I-bands (*I*) but not A-bands (*A*) or H-zone (H).

the hVLC-1 sequence since another TAMRA conjugated TAT-fusion peptide ^{TAMRA}TAT-p21, in contrast accumulated in the nucleolus and the cytoplasm of adult primary cardiomyocytes, rather than in the I-band and A-band of the myofibrils (not shown). Loading adult rat cardiomyocytes with hVLC-1-TAT^{TAMRA} (10 μM) did not change the resting sarcomere length, which were 1.91 ± 0.04 μm (n=40) without and 1.92 ± 0.04 μm (n=35) with hVLC-1-TAT^{TAMRA} (10 μM).

To elucidate the functional potency of N-terminal MLC-1 peptides in the whole intact heart, we generated transgenic rat (TGR) strains that expressed minigenes coding for the NH_2-terminal peptides 1–15 of the human atrial or ventricular MLC-1 sequence 1–15, namely, TGR/hALC-1/1–15 (L3966, L7475), and TGR/hVLC-1/1–5 (L6113, L6114), respectively. An α-MHC promoter of the rat was used to allow cardiomyocyte-specific transgene expression (**Fig. 3**). All TGR lines revealed a normal heart-to-body-wt ratio, normal life expectancy, and no obvious behavioral or physiological abnormalities.

Analysis of the transgene expression on the mRNA level was performed by RT-PCR (28 cycles). We observed comparable transgene mRNA levels in all TGR lines, with the exception of the TGR/hALC-1/1–15 (L7475), in which no RNA could be detected (Fig. 3).

The expressed mRNA levels of the TGR lines were also reflected in the peptide concentration on SDS-gel electrophoresis, Western blot, and specific reaction with peptide-directed antibodies raised against synthetic peptides hALC-1/3–15 or hVLC-1/3–15. Using synthetic peptides as standard, we calculated transgene expressions (expressed per mg SDS-soluble protein) of 42 ± 7 ng (6), 34 ± 5 ng (6), and 59 ± 10 ng (6) in

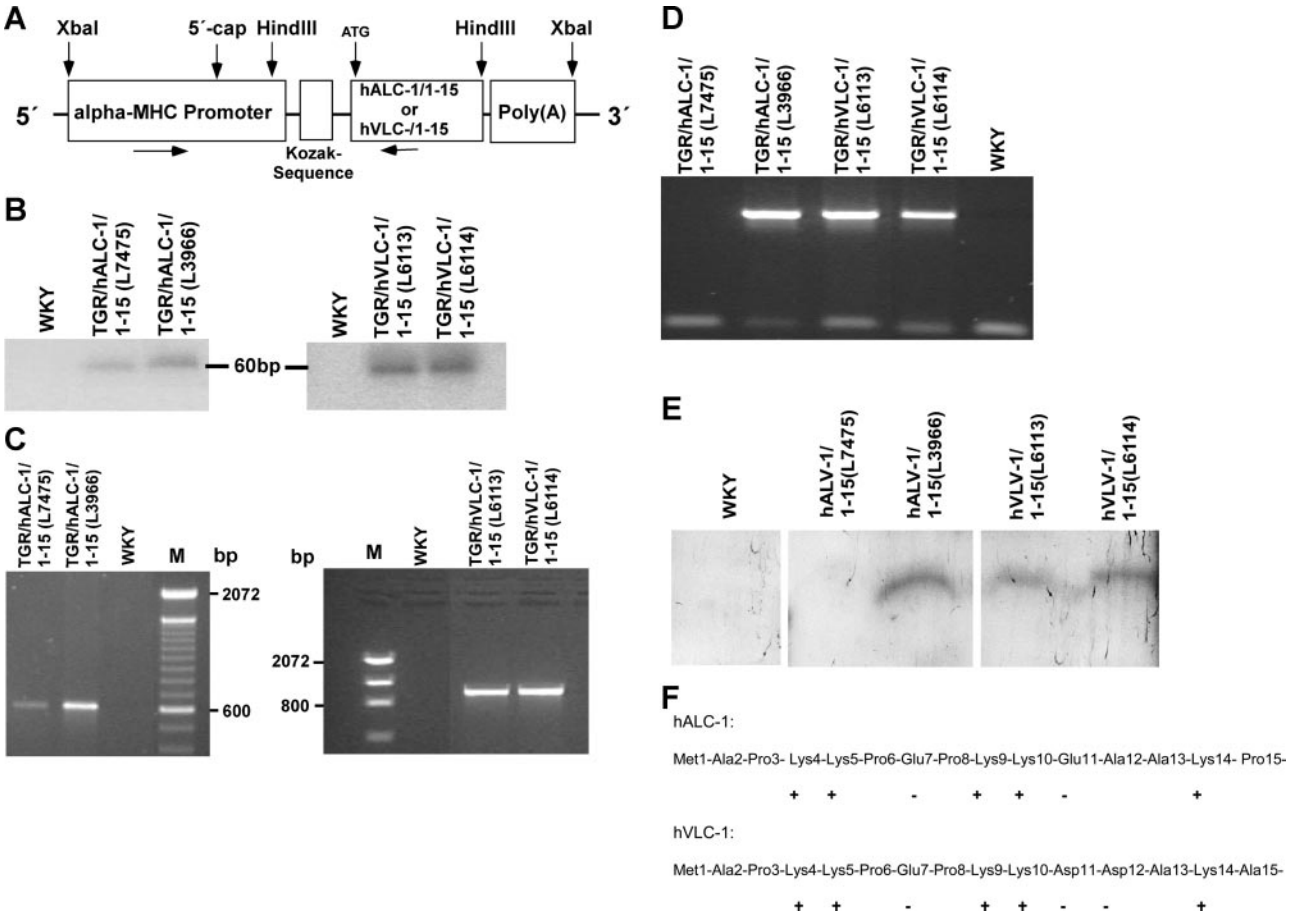

Figure 3. Generation and characterization of TGR. *A)* Schematic representation of the constructs used to generate the transgenic rat lines. The hALC-1/1–15 or hVLC-1/1–15 cDNA are linked to the α-MHC promoter via a Kozak sequence followed by the polyadenylation signal of SV40. Relevant restriction sites are represented on the diagram. Horizontal arrows indicate primers used for genotyping of the transgenic rats by PCR. *B, C)* Genotyping of transgenic rats. Genomic DNA from tail biopsies obtained from TGR/hALC-1/1–15 L7475 and L3966 (left) and TGR/hVLC-1/1–15 L6113 and 6114 (right) and nontransgenic WKY rats were analyzed by Southern blot (*B*) with *Hind*III-cut genomic DNA using a 60 bp probe as depicted in panel *A*) as well as transgene-specific PCR (*C*) (arrows in panel *A* correspond to the primer pairs used), yielding cDNA fragment of 606 bp and 807 bp in TGR/hALC-1/1–15 and TGR/hVLC-1/1–145, respectively. *D)* Semiquantitative analysis of cardiac mRNA expression. Cardiac RNA obtained from TGR/hALC-1/1–15 L7475 and L3966 (left) and TGR/hVLC-1/1–15 L6113 and 6114 (right) and nontransgenic WKY rats were analyzed by RT-PCR. *E)* Analysis of cardiac transgene expression on the peptide concentration. Cardiac MLC-1 peptides obtained from TGR/hALC-1/1–15 L7475 and L3966 (left) and TGR/hVLC-1/1–15 L6113 and 6114 (right), and nontransgenic WKY rats were analyzed by SDS-PAGE and Western blot. *F)* Amino acid sequence of the transgenic hALC-1 and hVLC-1 N-terminal peptides. Negatively and positively charged residues are labeled – and +, respectively.

TGR/hALC-1/1–15 (L3966), TGR/hVLC-1/1–5 (L6113), and TGR/hVLC-1/1–5 (L6114), respectively. No transgene expression could be observed in TGR/hALC-1/1–15 (L7475) (Fig. 3).

Assuming *1)* a relative MW of 1.5 kDa per peptide; *2)* ~150 μg SDS-soluble protein/mg muscle wet wt (unpublished observation), and *3)* 1 mg muscle wet wt = 1 mm^3 cell vol, we calculated ~4.2 μM, 3.4 μM, and 6 μM expressed transgenic peptides in TGR/hALC-1/1–15 (L3966), TGR/hVLC-1/1–5 (L6113), and TGR/hVLC-1/1–5 (L6114), respectively. For comparison, we calculated ~70 mM of MLC-1 in our cardiac preparations, assuming that 45% of SDS-soluble protein is myosin and 10% of myosin consists of MLC-1 (28 kDa).

Only those TGR lines that expressed peptide transgenes revealed a hypercontractile heart compared with nontransgenic controls (WKY rats). Left ventricular contractile parameters were determined using the electrically paced isolated perfused heart in Langendorff mode electrically paced at 340 bpm during steady-state contraction. In 3-month-old male TGR/hALC-1/1–15 (L3966), TGR/hVLC-1/1–5 (L6113), and TGR/hVLC-1/1–5 (L6114), developed systolic isovolumetric force as well as maximal rate of isovolumetric tension development and maximal rate of isovolumetric relaxation was significantly higher compared with their age-matched male WKY controls (**Fig. 4**). In contrast, an improvement of cardiac contraction could not be observed in TGR/hALC-1/1–15 (L7475), which expressed no detectable levels of the transgene on both the mRNA and peptide levels (cf. Fig. 3). The spontaneous (unpaced) heart rates were 225 ± 8 (12), 231 ± 7 (12), 242 ± 14, 222 ± 9 (12), and 233 ± 10 (12) in TGR/hALC-1/1–15 (L7475), TGR/hALC-1/1–15 (L3966), TGR/hVLC-1/1–5 (L6113), TGR/hVLC-1/1–5 (L6114), and WKY, respectively.

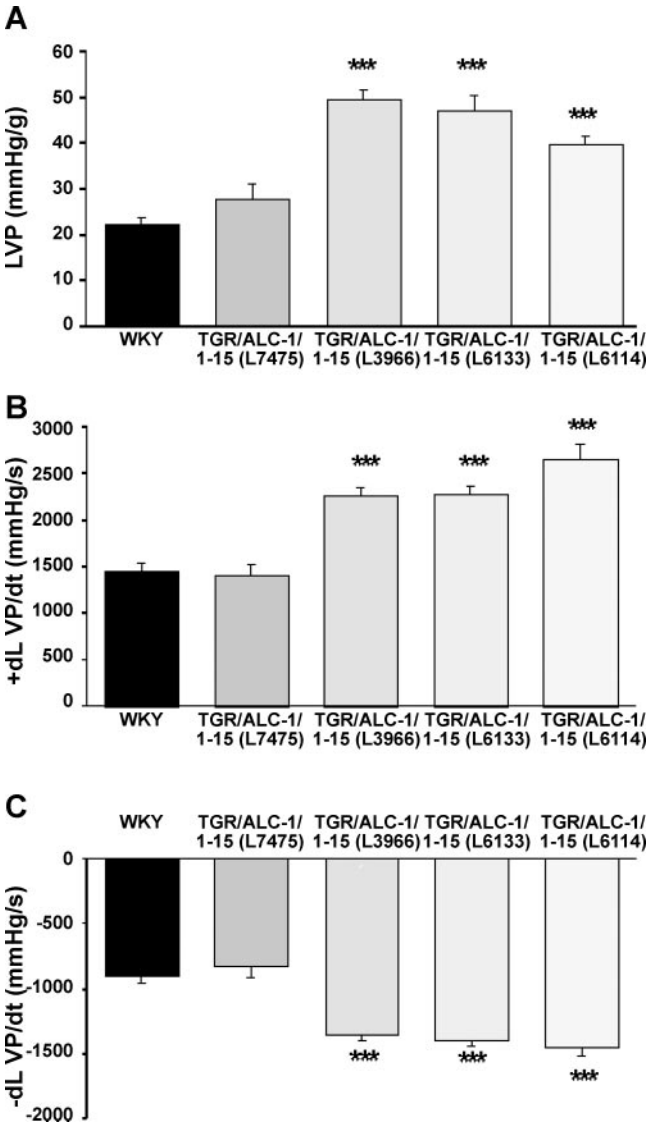

Figure 4. Functional properties of the hearts of 12-wk-old animals. Isolated perfused hearts (Langendorff mode) of TGR rat lines compared with the age-matching control (WKY) group. *A)* Developed left ventricular pressure (LVP). *B)* Maximum rate of pressure development (+dP/dt max). *C)* Maximum rate of pressure decrease (−dP/dt max) (relaxation rate). Values were expressed as means ± SE (n=12 animals per group), ***$P < 0.001$ TGR vs. WKY.

DISCUSSION

The kinetic properties of the myosin motor determines the contractile features of muscle. It has been demonstrated that the properties of myosin could be modulated by experimental manipulation of the interaction between actin and the NH_2 terminus of the essential myosin light chain (MLC-1): inhibition of the MLC-1/actin complex formation, i.e., by N-terminal MLC-1 peptides, accelerates the kinetic properties of the myosin motor molecule (14, 15) improved contractility of demembranated (skinned) cardiac fibers (25), and increased ATPase activity of myofibrils (26). These data suggest that N-terminal MLC-1 peptides have the capacity to improve the function of the whole intact heart.

To test this hypothesis, we generated transgenic rats (TGR) harboring minigenes encoding N-terminal MLC-1 peptides 1–15 of the human ALC-1 and VLC-1. Expressed transgenic peptides revealed the same mobility as the corresponding synthetic peptides. Since synthetic MLC-1 peptides with a N-terminal α-N-trimethylated alanine (Me_3Ala) revealed different mobilities in the SDS gel (unpublished observations), we conclude that the transgenic MLC-1 peptides are not subjected to the intracellular processings of endogenous MLC-1 isoforms, which are blocked by an N-terminal Me_3Ala (7).

We demonstrate for the first time here that the expression of minigenes encoding N-terminal domains of cardiac MLC-1 peptide isoforms significantly increased the intrinsic contractile state of the electrically stimulated, isolated perfused heart *ex vivo* of transgenic rats (TGR). This hypercontractile effect was not associated with cardiac hypertrophy. The spontaneous beating frequencies remained normal, suggesting that the pace-maker and electrical conduction system remained undisturbed in the hearts of all TGR lines investigated.

The TGR L7475, which did not express detectable amounts of transgene mRNA and peptide, revealed normal contractility parameters, demonstrating the specificity of the transgene action solely on the intrinsic contractile state of the heart.

The hypercontractile effect of N-terminal MLC-1 peptides was closely correlated with its actin binding capacity: both N-terminal human atrial and ventricular MLC-1 peptide isoforms specifically formed complexes with cardiac G-actin *in vitro* (14). The different dissociation constants of both MLC-1 peptides may reside in their different primary sequences, particularly in their different amounts of charged amino acid residues. In fact, experimental substitution of lysines by alanines (14, 24) demonstrated the functional importance of charged interactions between the NH_2 terminus of MLC-1 and actin.

Furthermore, the MLC-1 peptides seems to be tightly associated with the sarcomeres of the myofibrils in the living cardiomyocyte: by using synthetic TAMRA-conjugated transducible hVLC-1/1–15-TAT peptides and confocal microscopy of living adult primary rat cardiomyocytes, we detected fluorescence signals mainly in the actin-containing I-band (~65% of the fluorescence signals), and in the actin-myosin filament overlap zone (A-band; ~35% of the whole fluorescence signals). The actin binding information of N-terminal MLC-1 peptides seems to be so strong that it even dominated the nuclear translocation signal within the TAT sequence.

Binding of N-terminal MLC-1 peptides to sarcomeric actin both in the I-band but also within the actin-myosin overlap zone is a prerequisite for its functional effectiveness. Hence, the reported intracellular distribution pattern of N-terminal MLC-1 would predict not only improvements of shortening capacity, but also of isovolumetric force development, i.e., contractions without or with only small filament sliding that are elicited upon electrical stimulation of the isolated perfused Langendorff heart preparations. According to the lower A-band accumulation of the hVLC-1-TAT^{TAMRA} in resting primary cardiomyocytes, improvements of isovolumetric contractions would be less pronounced. However, the observed intracellular localization pattern obtained in resting primary cardiomyocyte incubated with hVLC-1-TAT^{TAMRA} for a few minutes may not precisely reflect the intracellular distribution of the transgenic peptides in the cardiomyocytes of the hearts of the TGR. The transgenic peptide is considerably smaller (~1.5 kDa) than the TAT-fused, TAMRA-conjugated VLC-1 peptide (~3.8 kDa), and may therefore penetrate the smaller lateral spacings within the actin-myosin filament overlap zone with a higher probability. Furthermore, the transgenic rat lines expressed the transgenes continuously for weeks. In addition, *in vivo* beating of the hearts with high frequencies may influence the intracellular distribution of the transgenic peptide. We, therefore cannot exclude the possibility that a higher fraction of the transgenic peptide accumulatesin the A-band *in vivo* than that observed in the confocal pictures obtained upon incubation of primary cardiomyocytes with hVLC-1-TAT^{TAMRA}, thus improving isovolumetric contraction more intensively.

Although hALC-1 and hVLC-1 peptide/actin interactions revealed different K_D values, we observed comparable hypercontractile states in TGR L3966, L6113, and L6114. This may be due to the fact that our Langendorff method as a contractility monitoring system could well resolve functional properties of hearts with and without transgene expression, but that it may not be sensitive enough to resolve functional differences of transgene-expressing animals based on different dissociation constants.

The expression levels of the transgenic peptides in the μM range observed in our TGR lines could be considered sufficient to induce an appropriate positive inotropic effect of the whole perfused heart. Indeed, even nanomolar concentrations of sticky MLC-1 peptides were sufficient to induce a significant increase in force and ATPase activity of *in vitro* muscle preparations (25, 26). It is not clear, however, whether the expression levels of transgenic peptides obtained with homogenized cardiac tissue also reflect peptide expression on the concentration of the single cardiomyocyte. In another TGR model in which we used the same genetic background (WKY rats) and the α-MHC promoter (36), we observed a mosaic expression of the transgene, i.e., a detectable transgene expression in only a fraction (~10%) of the cardiomyocytes of the heart. Considering the single cardiomyocyte, the reported transgene expression may therefore be underestimated by ~ one order of magnitude.

We recently hypothesized that binding of MLC-1 to actin via its sticky NH_2 terminus imposes an internal load to the myosin motor, resisting filament sliding and suppressing cross-bridge cycling rate (25). Relieving the myosin/MLC-1-actin tether by sticky MLC-1 peptides, which compete with MLC-1 for actin binding, decreases internal load and speeds up cross-bridge function, thus improving chemomechanical energy transformation and hence muscle function. In fact, since an increased maximal shortening velocity equals an increased rate of cross-bridge detachment (31), the improved isovolumetric relaxation rate observed upon inhibition of the myosin/MLC-1-actin tether by sticky MLC-1 peptides in the hearts of TGR could well be explained by a direct modulation of the cross-bridge cycle rate (increased detachment rate constant g_{app}).

Besides a competitive effect on the cross-bridge cycling kinetics, we propose a mimetic action of sticky MLC-1 peptides: tropomyosin increased the affinity of N-terminal MLC-1 peptides to F-actin whereas binding of troponin I abolished MLC-1 peptide binding to F-actin-tropomyosin (19, 27). Ca^{2+} binding to troponin C reduces actin affinity of troponin I (28) and may therefore lose its inhibitory effect on MLC-1 binding to actin during muscle activation. Thus, upon actin binding, MLC-1 peptides may raise the thin filament activation concentration by a reciprocal coupling mechanism, which could increase the probability of actin-

myosin interaction, i.e., increased rates of cross-bridge attachment and force generation (f_{app}). The rate of redevelopment of isometric tension rose if the sum of $f_{app} + g_{ap}$ increases (32). This could then explain the significant increase of the maximal rate of isovolumetric force generation of the hearts of TGR. In fact, the low transgenic peptide/endogenous MLC-1 ratio observed in our TGR lines suggests a more dominant role of the peptides mimetic features as the main mechanism of action of the positive inotropic effects of the N-terminal MLC-1 peptides in our TGR lines.

The hypercontractile effect of sticky MLC-1 peptides seems to be independent of the calcium activation concentration of the cardiomyocyte, i.e., a calcium-sensitizing mechanism. From a comparative proteome analysis of a previous TGR model that overexpressed the whole human ALC-1 gene under the control of the same α-MHC promoter (36), we suggest that the protein expression pattern besides the transgene expression of the TGR lines investigated here remain normal, and no changes of the calcium handling system could be expected. In fact, sticky MLC-1 peptides could increase isometric force of skinned fibers (25) and ATPase activity of myofibrillar preparations (26) at clamped free calcium concentrations.

In conclusion, we demonstrated for the first time that sticky N-terminal MLC-1 peptides bind to cardiac actin *in vitro* as well as to the sarcomeres of the myofibrils in the living cardiomyocyte and improved the contractility of the whole isolated perfused heart. The positive inotropic mechanism of sticky MLC-1 peptides is suggested to rely on Ca^{2+} independent improvements of the myofibrillar activation and myosin motor function—a new therapeutic approach for the treatment of heart failure that is beyond the manipulation of the calcium handling system, i.e., the strategy of most conventional treatments of heart failure. FJ

This work was supported by DFG Mo 362/22–1 (to I.M.) and MDC QPB C03/09 (to C.C.). We thank Dr. Ursula Ganten and Prof. Dr. M. Bader, MDC, Berlin, Germany, for supporting the experimental work and valuable advices. This work is dedicated to my (I.M.) former academic teacher Prof. Dr. Johann Caspar Rüegg, who already used peptides as tools in muscle research some decades ago.

REFERENCES

1. Abraham, W. T., and Bristow, M. R. (1997) Specialized center for heart failure management. *Circulation* **96,** 2755–2757
2. Konstam, M. A. (2000) Progress in heart failure management? Lessons from the real world. *Circulation* **102,** 1076–1078
3. Geeves, M. A., and Holmes, K. C. (1999) Structural mechanism of muscle contraction. *Annu. Rev. Biochem.* **68,** 687–728
4. Rayment, I., Rypniewski, W. R., Schmidt-Base, K., Smith, R., Tomchick, D. R., Benning, M. M., Winkelmann, D. A., Wesenberg, G., and Holden, H. M. (1993) Three-dimensional structure of myosin subfragment-1: a molecular motor. *Science* **261,** 50–58
5. Winstanley, M. A., Trayer, H. R., and Trayer, I. P. (1977) Role of the myosin light chains in binding to actin. *FEBS Lett.* **77,** 239–242
6. Prince, H. P., Trayer, H. R., Henry, G. D., Trayer, I. P., Dalgarno, D. C., Levine, B. A., Cary, P. D., and Turner, C. (1981) Proton nucleart-magnetic-resonance spectroscopy of myosin subfragment 1 isoenzymes. *Eur. J. Biochem.* **121,** 213–219
7. Henry, G. D., Trayer, I. A., Brewer, S., and Levine, B. A. (1985) The widespread distribution of a-N-trimethylalanine as the N-terminal amino acid of light chains from vertebrate striated muscle myosins. *Eur. J. Biochem.* **148,** 75–82
8. Labbe, J. P., Audemard, E., Bertrand, R., and Kassab, R. (1986) Specific interactions of the alkali light chain 1 in skeletal myosin heads probed by chemical cross-linking. *Biochem.* **25,** 8325–8330
9. Timson, D. J., Trayer, H. P., and Trayer, I. P. (1998) The N-terminus of A1-type myosin essential light chains bind actin and modulates myosin motor function. *Eur. J. Biochem.* **255,** 654–662
10. Abillon, E., Bremier, L., and Cardinaud, R. (1990) Conformational calculations on the Ala14-Pro27 LC1 segment of rabbit skeletal myosin. *Biochim. Biophys Acta* **1037,** 394–400
11. Bhandari, D. G., Levine, B. A., Trayer, I. P., and Yeadon, M. E. (1986) H-NMR study of mobility and conformational constraints within the proline-rich N-terminal of the LC-1 alkali light chain of skeletal myosin. *Eur. J. Biochem.* **160,** 349–356
12. Fodor, W. L., Darras, B., Seharaseyon, J., Falkenthal, S., Francke, U., and Vanin, E. F. (1989) Human ventricular/slow twitch myosin alkali light chain gene characterization, sequence, and chromosomal location. *J. Biol. Chem.* **264,** 2143–2149
13. Seharaseyon, J., Bober, E., Hsieh, C. L., Fodor, W. L., Francke, U., Arnold, H. I. H., and Vanin, E. F. (1990) Human embryonic/atrial myosin alkali light chain gene: characterization, sequence, and chromosomal location. *Genomics* **7,** 289–293
14. Timson, D. J., Trayer, H. R., Smith, K. J., and Trayer, I. P. (1999) Size and charge requirements for kinetic modulation and actin binding by alkali 1-type myosin essential light chains. *J. Biol. Chem.* **274,** 18271–18277
15. Hayashibara, T., and Miyanishi, T. (1994) Binding of the amino-terminal region of alkali1 light chain to actin and its effect on actin-myosin interaction. *Biochem.* **33,** 12821–12827
16. Sutoh, K. (1982) Identification of myosin-binding sites on the actin sequence. *Biochemistry* **21,** 3654–3661
17. Trayer, I. P., Trayer, H. R., and Levine, B. A. (1987) Evidence that the N-terminal region of A1-light chain of myosin interacts directly with the C-terminal region of actin. A proton magnetic resonance study. *Eur. J. Biochem.* **164,** 259–266
18. Weeds, A.G., and Taylor, R. S. (1975) Separation of subfragment-1 isoenzymes from rabbit skeletal muscle myosin. *Nature (London)* **257,** 54–56
19. Trayer, H. R., and Trayer, I. P. (1985) Differential binding of rabbit fast muscle myosin light chain isoenzymes to regulated actin. *FEBS Lett.* **180,** 170–174
20. Moore, J. R., Dickibnson, M. H., Vigoreaux, J. O., and Maughamn, D. W. (2000) The effect of removing the N-terminal extension of the Drosophila myosin regulatory light chain upon flight ability and the contractile dynamics of indirect flight muscle. *Biophys. J.* **78,** 1431–1440
21. Chalovich, J. M., Stein, L. A., Greene, L. E., and Eisenberg, E. (1984) Interaction of isozymes of myosin subfragment 1 with actin: effect of ionic strength and nucleotide. *Biochem.* **23,** 4885–4889
22. Lowey, S., Waller, G., and Trybus, K. M. (1993) Function of skeletal muscle myosin heavy and light chain isoforms by an in vitro motility assay. *J. Biol. Chem.* **268,** 20414–20418
23. Bottinelli, R., Betto, R., Schiaffino, S., and Reggiani, C. (1994) Unloaded shortening velocity and myosin heavy chain and alkali light chain isoform composition in rat skeletal muscle fibers. *J. Physiol. (London).* **478,** 341–349
24. Sweeney, H. L. (1995) Function of the N terminus of the myosin essential light chain of vertebrate striated muscle. *Biophys. J.* **68,** 112s–119s
25. Morano, I., Ritter, O., Bonz, A., Timek, T., Christian, F., and Michel, V. G. (1995) Myosin light chain-actin interaction regulates cardiac contractility. *Circ. Res.* **76,** 720–725
26. Rarick, H. M., Opgenorth, T. J., von Geldern, T. W., Wu-Wong, J. R., and Solaro, R. J. (1996) An essential myosin light chain peptide induces supramaximal stimulation of cardiac myofibrillar ATPase activity. *J. Biol. Chem.* **271,** 27039–27043
27. Patchell, V. B., Gallon, C. E., Hodgkin, M. A., Fattoum, A., Perry, S. V., and Levine, B. A. (2002) The inhibitory region of troponin

I alters the ability of F-actin to interact with different segments of myosin. *Eur. J. Biochem.* **269,** 5088–5100
28. Rüegg, J. C. (1986) Calcium in muscle activation. Springer-Verlag, New York
29. Stepkowski, D. (1995) The role of the skeletal muscle myosin light chains N-terminal fragments. *FEBS Lett.* **374,** 6–11
30. Nieznanski, K., Nieznanska, H., Skowronek, K., Kasprzak, A. A., and Stepkowski, D. (2003) Ca^{2+} binding to myosin regulatory light chain affects the conformation of the N-terminus of essential light chain and its binding to actin. *Arch. Biochem. Biophys.* **417,** 153–158
31. Huxley, A. F. (1957) Muscle structure and theories of contraction. *Prog. Biophys. Biophys. Chem.* **7,** 255–318
32. Brenner, B. (1988) Effect of Ca^{2+} on cross-bridge turnover kinetics in skinned single rabbit psoas fibers: implications for regulation of muscle contraction. *Proc. Natl. Acad. Sci. USA* **85,** 3265–3269
33. Behlke, J., Ristau, O., and Schönfeld, H. J. (1997) Nucleotide-dependent complex formation between the *Escherichia coli* chaperonins GroEL and GroES studied under equilibrium conditions. *Biochemistry* **36,** 5149–5156
34. Fujita, H. (1962) Mathematical Theory of Sedimentation Analysis. Academic Press, New York
35. Mullins, J. J., Peters, J., and Ganten, D. (1990) Fulminant hypertension in transgenic rats harbouring the mouse Ren-2 gene. *Nature (London)* **344,** 541–544
36. Abdelaziz, I. A., Segaric, J., Bartsch, H., Petzhold, D., Schlegel, W. P., Kott, M., Seefeld, I., Klose, J., Bader, M., Haase, H., and Morano, I. (2004) Functional characterization of the human atrial essential myosin light chain (hALC-1) in a transgenic rat model. *J. Mol. Med.* **82,** 265–274

Received for publication November 16, 2005
Accepted for publication December 28, 2005